hydroelectric power plants
International Course on Hydroelectric Power Plants
Coimbra, Portugal, July, 1995

8. SHAPE OPTIMIZATION OF DAMS FOR STATIC AND DYNAMIC LOADING

Luís M.C. Simões
Department of Civil Engineering, University of Coimbra, 3049 Coimbra Codex, Portugal

ABSTRACT This lecture concerns the use of algorithms to find the optimal boundary description of dams. Several components of the CAD tool such as shape representation, structural analysis, optimization procedure and sensitivities of the responses with respect to design-variable changes are described with detail. Illustrative examples are given showing the applicability of the proposed method.

In Memoriam

JOSÉ SIMÕES

1. INTRODUCTION

The decision to build a dam would include consideration of some or all of the following: (a) The value of the reservoir capacity that is a function of the irrigation, domestic, recreational and power generation demands; (b) The value of the dam as an essential element for flood control which can be expressed as a function of the dam height; (c) The cost of the reservoir (excluding the dam structure) which may also be formulated in terms of dam height; (d) The cost of the dam structure.
In this study, it is not intended to include all the factors affecting the economics of a design, eg: construction material, discharge safety equipment (spillways, outlet works, etc.). The problem is to determine some or all of the following: (a) the shape and location (within a given area) (b) the height (c) the construction materials' properties (eg: elastic modulus, concrete strength) of a dam in order to maximize merit functions expressing the cost and functional usefulness of the structure in the terms given, subject to practical constraints on the behaviour and geometry. The cost of a dam is a function of such components as area of formwork, volume of excavation and volume of concrete. The latter component is often a dominant factor in the determination of cost.
Concrete dams have either a fundamentally 2D behaviour (massive, hollow and buttress gravity dams) or resist by thrust action (arch gravity, single and multiple arch dams) in which case a 3D analysis model is usually employed. Roller compacted concrete is a recent trend in dam construction. The choice of the dam type depends on a number of factors ranging from environmental conditions (topographical, geological and geotechnical, hydrologic and hydraulic), design and construction methods to economic issues. The shape of the valley which often determines the choice from arch (for V shaped valleys), mixed gravity-arch and multiple arch (U shaped), gravity (for trapezoidal cross section) will not be discussed here.
Generally dams are designed by trial and error, that is an initial scheme is proposed and then analysed. If it satisfies the demands of the design specifications, the scheme is adopted. Otherwise, the shape of the dam is modified and reanalyzed. The shape obtained in this way is feasible but not necessarily optimal or even good. Moreover, the time for design is rather long.
The design of dams is fundamentally a configuration optimization problem, where the external geometry of the structure is to be determined. The optimal design problems can be stated in a mathematical programming form with geometric design variable representing coordinates of the nodes or boundaries of elements. A feature of the problem is that there arerelatively few significant shape design variables. Each design stage of the

shape optimization process presented here involves: (1) analysis of an initial or trial design by finite element analysis; (2) use of sensitivity analysis and approximation concepts to formulate the performance constraints as explicit linear functions of design variables; (3) optimization by means of an efficient optimization algorithm to obtain a better solution. The new design then becomes the trial design for the next design iteration and the process is continued until the change in design over a number of successive stages is less than some specified tolerance. Since within the iterative process the shapes vary continuously, careful consideration has to be given to describe the changing boundary shape in order to employ an adequate finite element mesh and obtain accurate sensitivity analysis results.

Penalty function methods have been applied by Ramakrishnan and Francavilla (1975) and by Vitiello (1973) to the shape optimization of hollow gravity and solid gravity dams, respectively. In both papers a two dimensional finite element analysis model is used. Early research investigations into the problem of arch dam design have dealt mainly with membrane type solutions (Fialho,1955). Although these methods ignore foundation elasticity and bending stresses, and consider a single loading condition (water pressure and the weight of concrete), they may provide useful starting points for more comprehensive studies. Difficulties in eliminating tensile stresses (even under a single loading case) were experienced (Sharpe, 1969) when using thin shell theory to optimize a doubly curved arch dam with Ritter's algorithm. More recent results for the three-dimensional shape optimization of arch dams use a sequential linear programming algorithm associated with either 8 node (Wassermann,1983-84) or 20 node (Ricketts and Zienckiewicz,1984) isoparametric elements. To date, shape optimization has not been applied to actual dams except in China (Zhu Bofang, 1987).

2. SHAPE REPRESENTATION

The suitability of the geometrical model is highly important for the optimum design of arch dams. The model must correspond with the stress state of the arch dam, aiming towards fully developing the potential of the structure and rationally utilizing the strength of materials. On the other hand, to facilitate construction, the geometric model should not be complicated, otherwise it cannot easily be adopted in the project.

2.1 Gravity Dams

Control nodes are used to define the coordinates of the boundary nodes and their moving directions. The geometry of a concrete gravity dam shown in Figure 1 is described by 3 or 5 design (shape) variables.

Fig. 1 Shape Variables

x_1, x_2 and x_3 give the location of the cross sections bottom left, top left and top right, respectively, with respect to the starting shape of the dam. The position of the bottom right of the downstream face is fixed. x_4 and x_5 are the tangents at the bottom left and right of the heel, respectively. Although the upstream and downstream faces may have parabolic shapes if the last two design variables are used, the boundary is approximated by piecewise linear functions.

2.2. Arch Dams

The way to describe the shape of the arch dam is the key element in the process of obtaining the optimal shape. The boundary shape will be described in this section by piecewise continuous functions. To describe the model geometrically, the V shaped valley depicted in Fig.2 is divided into seven layers along its elevation, and the contour lines of the usable rock on both sides are represented by seven broken lines, the nodal coordinates of which are the original data input. The upstream face of the dam may define either a single-curvature or double-curvature surface. The horizontal section of the dam may be ne of the following types: single-centered arc, multicentred arc, parabola, ellipse, hyperbola, or logarithmic spiral.

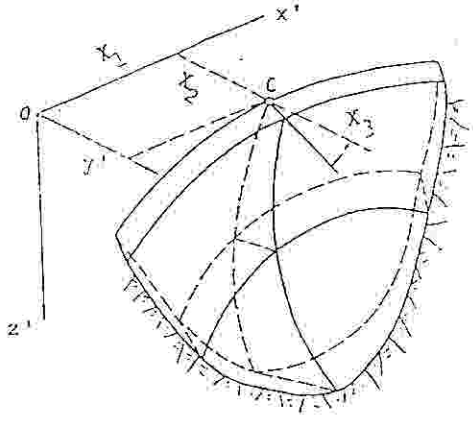

Fig. 2 Arch Dam

To determine the shape of an arch dam, the central vertical section is determined first, and then the shape of the horizontal sections at various elevations is obtained. Three methods may be used to find the shape of the vertical and horizontal sections: (1) get the function of the upstream and downstream boundaries, (2) get the function of the upstream boundary and the thickness of the section; and (3) get the function of the central line of the section and its thickness. The second method is more widely used used to establish the shape of the central vertical section of the dam, in which case the design parameters are the curve of the upstream boundary and the thickness. These design parameters vary with the coordinate z and may be expressed by polynomials as follows:

$$f(z) = k_0 + k_1 z + k_2 z_2 + \ldots + k^m z_m \qquad (1)$$

where k_0, k_1, k_2, ..., km are design variables. As illustrated in Fig.2, the horizontal coordinates of point C (the top of the upstream face of the central vertical section) are the global coordinates x_1 and x_2. The angle between the radial plane of the central vertical section and the Y0Z plane is x_3. These three design variables define the position of the dam axis that may shift and turn in the process of optimization. Altogether, there are n

design variables, where x_1, x_2 and x_3 find the position of the dam axis and x_4, x_5, ...,x_n determine the shape of the dam.

Shape of the Central Vertical Section

For a cylindrical arch dam, the upstream boundary of the central vertical section is generally a vertical straight line; and only one polynomial of nth order, is needed to determine the thickness of the section.

For the central vertical section of a double-curvature arch dam, as shown in Fig.3a, one polynomial of nth order is used to determine the curve of the upstream boundary or the central line of the section and another polynomial is used to determine the thickness.

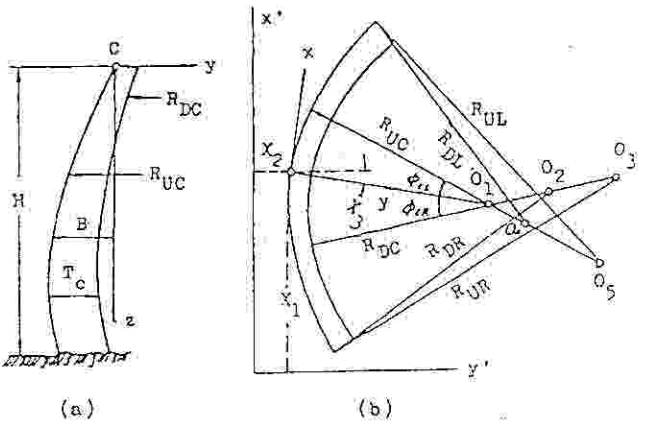

Fig. 3 Five centered Double Curvature Arch Dam a) Central Vertical Section b)Horizontal Section

Shape of the Horizontal Section

The shape of the horizontal section of the dam may be one of the following six types: in a single-centered arch dam, the horizontal section has a constant radius of curvature and a constant thickness; R_u, the radius of the upstream face and T_c, the thickness of the section, are expressed by two polynomials of z.

In a multicentered arch dam, the horizontal section of the dam may have from two to five centers of curvature. Its, it is shown below how to determine the shape of a five-centered, double-curvature arch dam. The horizontal section includes three segments of arcs; the central arc has a constant thickness, while the two lateral arcs are of variable thickness and their upstream and downstream faces have different centers and radii of curvature. From Fig.3b it is clear that the horizontal section is completely determined by the eight design parameters R_{uc}, T_c, O_1O_3, O_2O_3, O_1O_5, O_4O_5, ϕ_{cr} and ϕ_{cl}. Generally the first six parameters are expressed as polynomials of third order and the last two parameters are expressed by two of first order polynomials. The shape of arch dams with two to four centers may be derived from the five-centered arch dam mentioned above. For example, if $O_2O_3=O_4O_5=0$ a three-centered arch dam is defined, the horizontal section of which is an arch of three segments of constant thickness with three different radii.

As shown in Fig.4a, the axis of the arch of a parabolic dam is expressed by two parabolas as follows.

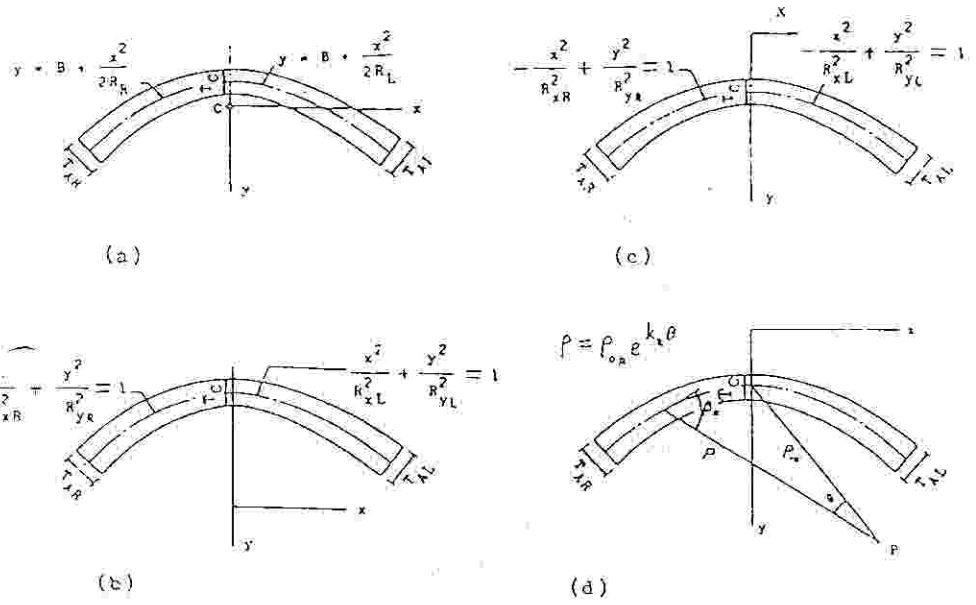

Fig. 4 Horizontal Sections of Noncircular Dams a) Parabolic b) Elliptical c) Hyperbolic d) Logarithmic Spiral

For the right half:

$$y = B + \frac{x^2}{2R_r} \tag{2a}$$

and for the left half,

$$y = B + \frac{x^2}{2R_r} \tag{2b}$$

where B is the y-coordinate of the crown; R_r and R_l are the radii of curvature of the right and left halves at x = 0. The thickness of the horizontal section is expressed as follows. For the right half:

$$T(s) = T_c + (T_{ar} - T_c)\frac{s^2}{s_{ar}^2} \tag{3a}$$

and for the left half,

$$T(s) = T_c + (T_{al} - T_c)\frac{s^2}{s_{al}^2} \tag{3b}$$

in which T_c, T_{ar} and T_{al} are thicknesses of the arch at crown, right and left abutments, respectively; s is the length of arc from the crown, sar and sal are length of arc at the right

and left abutments, respectively, and T_c, T_{ar}, T_{al}, R_r and R_l are the design parameters that determine the shape of a parabolic dam. If all these design parameters are expressed by polynomials of nth degree, the total number of design variables is n=8+6m. If m = 2, 3 or 4, n will be 20, 26, and 32, respectively. The number of design variables is smaller in the case of symmetrical dams.

The axis of the arch of the elliptical dam shown in Fig.4b is expressed by two ellipses and the thickness is again, expressed by (3). The design parameters determining the shape of the dam are Rxl, Ryl, Rxr, Ryr, B, Tc, Tar and Tal. The total number of design variables is n=10+8m. The axis of the arch of the hyperbolic dam shown in Fig.4c is expressed by two hyperbolas, and the thickness by (3), n=10+8m.

The axis of the arch of the logarithmic spiral dam shown in Fig.4d is expressed as follows. For the right half:

$$\rho = r_{o\rho}\, e^{k_r \theta} \tag{4a}$$

and for the left half,

$$\rho = \rho_{ol}\, e^{k_l \theta} \tag{4b}$$

where ρ = radius vector; and θ = polar angle. The thickness is expressed by (3). The design parameters are ρ_{or}, ρ_{ol}, k_r, k_l, B, T_c, T_{ar} and Tal. If k_r and k_l are expressed by linear equations of z and the remaining design parameters expressed by polynomials of nth order of z, then n=12+6m. To improve stress conditions in some regions it is sometimes better to include extra variables allowing for a variation of thickness T_i at the ith point, the upstream coordinate z_j of the jth point and radius of curvature R_k at the kth point. From past experience, based on trial load calculations for five centered arch dams, the parabolic and the logarithmic spiral shape lead to a reduction of the volume of concrete needed. Moreover, the latter gives a larger margin of safety than the other designs, if the same volume of material is used and is therefore recommended.

3. STRUCTURAL ANALYSIS

The finite element techniques, taking into account plane strains, soil interaction, thermal stresses, etc. are now current practice for dam design and can be used in the optimization process. The static structural analysis consists of solving the equilibrium equations

$$K\,u = P \tag{5}$$

where K is the structural stiffness matrix, formed by assembling all elements stiffness matrices K_e, u is the unknown nodal displacement matrix and P the generalized load vector including the weight of the structure itself, hydrostatic pressure or thermal loads. Both K and P are functions of the shape design variables x_i. Given the nodal displacements, a structural response R can be related to them through matrix Q:

$$R = Q\,u \tag{6}$$

The stress matrix at a given point can also be written as:

$$\sigma = S_e\, u_\epsilon \tag{7}$$

where Se is the element stress matrix depending on the element nodal forces and the element stiffness matrix; ue is the element nodal displacements.

When the optimization requires function evaluation a complete finite element analysis is performed. However, because the actual configuration of the structure is changing, the finite element generated for the initial configuration may not be adequate throughout the design process. Therefore, it is necessary to provide automatic mesh generation capability within the finite element analysis program to ensure that the analysis results are always meaningful. Because a detailed analysis is required at each step in the optimization process, the problem should be formulated to reduce computational effort. One attractive approach to this is to begin the design with a relatively coarse finite-element mesh. As the optimization progresses, the mesh is refined in areas of high stress concentration so that as the optimum is approached the f.e. model is detailed enough to ensure reasonable accuracy.

3.1 Gravity Dams

The finite element idealization for the system shown in Figure 2 consists of 18 quadrilateral elements and 77 nodes, which provide 154 degrees of freedom (90 in the dam and 64 on the foundation). This mesh was refined to 72 quadrilateral elements (40 in the dam and 32 in the foundation) for the final shape to ensure that the response of the model was meaningful.

3.2 Arch Dams

Because the allowable stresses in the design specifications are primarily derived from the experiences of arch dams designed by the trial load method in the past 60 years, the trial load method is still in use in many countries. Owing to the stress concentration, the stresses in arch dams calculated by FEM are generally greater than those calculated by the trial load method.

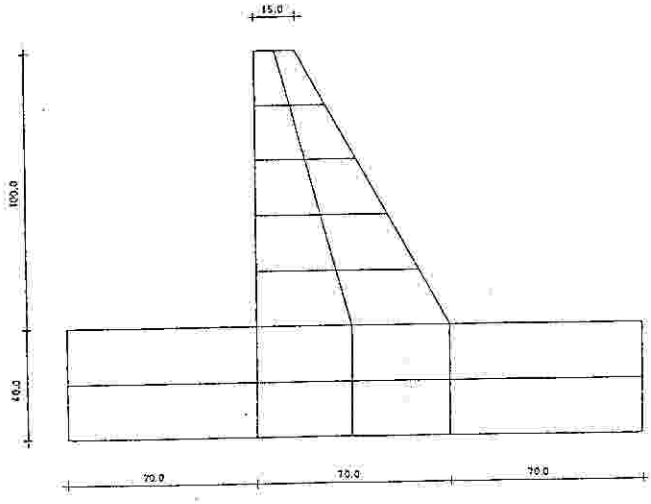

Fig. 5 Finite Element Mesh

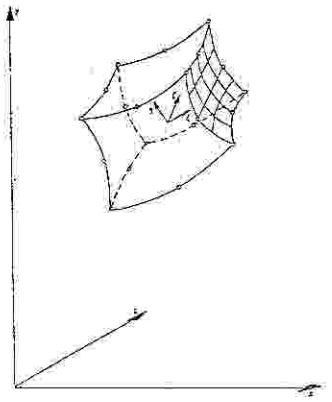

Fig. 6 3D Isoparametric finite element with 20 nodes

Finite elements results for the Alvito dam (mesh made of 20 node brick elements and the loading condition consisting of water pressure and self-weight)

	N° elements
A : Finite element mesh without foundation interaction (dam clamped on a rigid valley)	9
B: Finite element mesh without foundation interaction (dam clamped on a rigid valley)	16
C : Finite element mesh without foundation interaction (dam clamped on a rigid valley)	25
D : Finite element mesh with foundation interaction (complete dam-foundation system)	9 + 14
E : Finite element mesh with foundation interaction on the downstream side	9 + 8

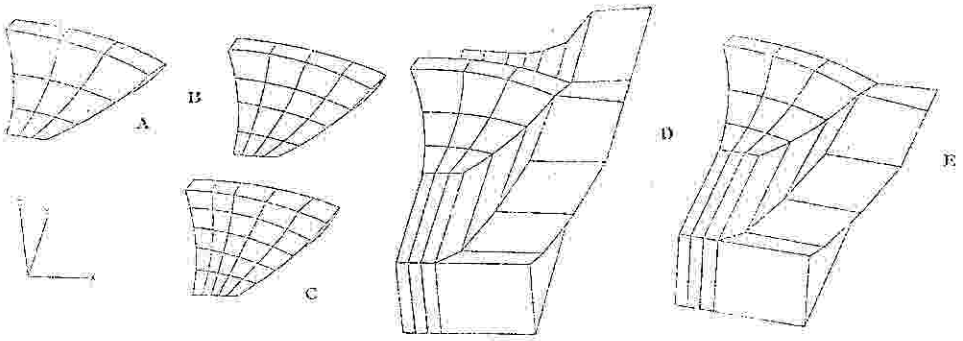

Fig. 7 Finite Element Mesh corresponding to models A-E

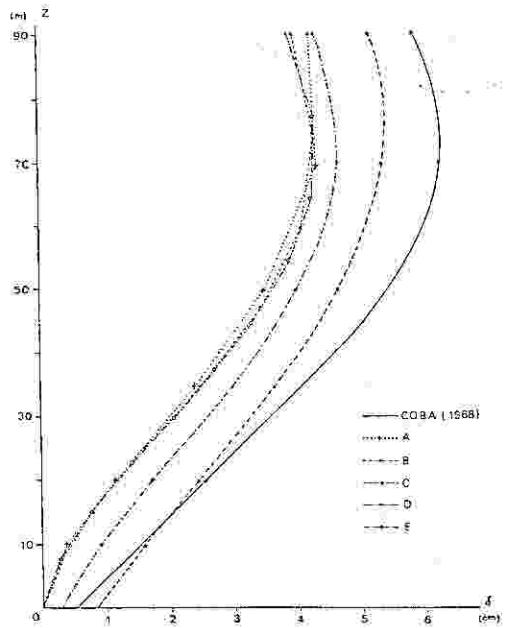

Fig. 8 Normal displacements at the central crown cantilever

From the results of Fig. 2 and 3 it may be concluded that no advantage can be gained from using more than 9 elements to model the concrete dam. Models A and C were also tested for the 8 node brick element. The errors involved in evaluating the normal displacements of the crest profile were 163% and 15%, respectively.

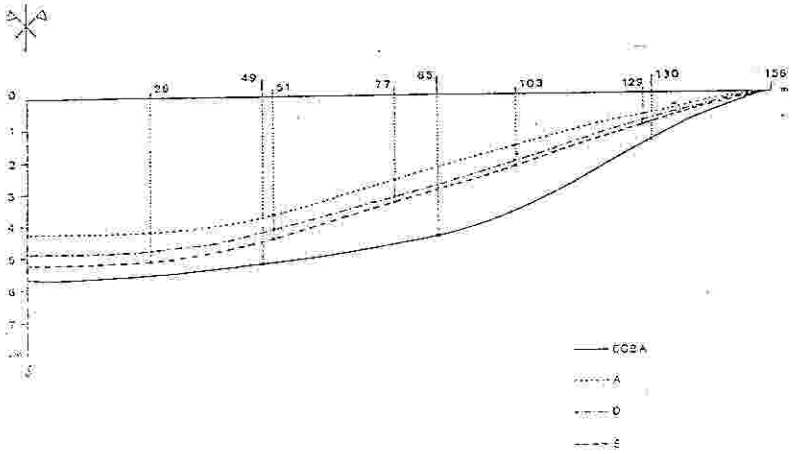

Fig. 9 Radial displacements at the crest profile

3.3 Dynamic Response

When the ground motion history from an earthquake is considered as support excitation for the structure, either modal analysis or step-by-step integration procedures must be used for computing the dynamic response analysis. The earthquake response should include dam-reservoir and dam-foundation interaction. The equations of motion at time t are:

$$M\,\ddot{u}(t) + C\,\dot{u}(t) + K\,u(t) = P(t) \tag{8}$$

where M, C, and K are functions of time or constants in linear systems, while they are also functions of displacements, velocities, etc. in non-linear systems.
The modal superposition method can used to compute dynamic displacements and stresses in linear elastic systems. This analysis involves solving the system of undamped dynamic equilibrium equations that can be reduced to the eigenvalue equation:

$$K\,\varnothing_r - \lambda_r M\,\varnothing_r = 0 \tag{9}$$

where $\varnothing_r$ is an eigenvector corresponding to the rth eigenvalue λ_r.
The step-by-step integration technique is suitable for both linear and non-linear systems. The response is evaluated for a series of short time increments, δt, generally taken of equal length for computational convenience and selected to be about one-sixth of the shortest natural period of the structure. Among step-by-step integration techniques, Newmark β method is widely used.

3.4 Hydrodynamic pressures

Associated with earthquakes, the design loads for dams include water pressure in addition to the hydrostatic pressures. The additional water pressures associated with horizontal earthquake motion in the standard design loads, based on assumptions of rigid dam and incompressible water, underestimate the importance of the hydrodynamic effects in the response of concrete gravity dams, although in arch dams the differences are not significant. The basic problem of hydrodynamic pressures on dams during earthquakes was first solved analytically by Westergaard in 1933 for vertical upstream faces. Chwang and Housner (1978) extended the momentum balance method developed by Von Karman also in 1933 to obtain pressures on dams with inclined faces. A more accurate semi-analytical solution for hydrodynamic pressure destribution on dams with arbitrary upstream faces is used here (Tsai, 1992). The compressibility of the water is included in the formulation. The pressure distributions in the fluid domain are expressed as the sum of functions with amplitude coefficients that satisfy all boundary conditions except at the upstream face of the dam. These coefficients are determined by using least (or Galerkin) squares so that the residual error is minimized.

4. OPTIMIZATION

4.1 Minimum Cost Model

Objective Function

The objective function is the cost of the dam, which may be expressed as the sum of the cost of concrete in the dam body plus the cost of foundation excavation. Generally, the cost of foundation excavation is much less than that of dam concrete, so the volume of dam concrete is usually used as the objective function. Constraint conditions include

geometry, stress and stability, which should satisfy the demands of design specifications and take into account the requirements of structural arrangement and construction.

Geometrical Constraints

The range in which the dam axis shifts are specified according to geological and topographical conditions. Depending on traffic requirements, the minimum width of the crest is then decided. Sometimes the maximum width of the base of the dam is limited to control the length of construction block. To facilitate construction, the maximum slope of overhang at the upstream and downstream faces should also be controlled.

Stress Constraints

Arch dams are constructed of mass concrete without reinforcement and are designed according to allowable principal stesses. Under the hydrostatic pressure, silt pressure, temperature changes and dead loads, the stresses should not exceed the admissible values specified. Before the grouting of contraction joints, the tensile stress caused by the dead load in construction blocks of different heights (corresponding to different stages of construction) should be controlled within the range of allowable values for safety during construction.

Stability Constraints

In the light of the importance of the dam and geological conditions, the constraints ensuring the sliding stability of the dam may be expressed by limiting the coefficient of sliding stability, the angle of thrust at the abutment (in the case of arch dams), the central angle of the arch (arch dams) and overturning moment (gravity dams). Some empirical conditions proposed by the design engineers but not included in the design specifications must also be considered.
This formulation leads to a nonlinear mathematical programming problem which can be solved by the penalty function method or by sequential programming with linear or quadratic approximations of the objective function.

4.2 Maximum Safety Model

Alternatively, the stress field can be optimized: maximum compressive stresses in most of the volume and minimum tensile stresses subject to constraints on the cost and overall stability of the dam.

4.3 Multi-objective formulation

Pareto's economic principle is gaining increasing acceptance in relation to multi-objective optimization problems. In minimization problems a solution vector is said to be "Pareto optimal" if no other feasible vector exists that could decrease one objective function without increasing at least one other. The optimum vector usually exists in practical problems and is not unique. The volume of the dam is the sum of the volumes of the finite elements,

$$V = \Sigma_e v_e \tag{10}$$

where e is the index of a finite element in the dam. A second set of goals arises from the requirement that the stresses should be as small as possible:

$$\sigma(x) \leq \sigma^u \qquad \sigma(x) \geq -\sigma^l \tag{11}$$

where σ^u and σ^l are tensile and compressive admissible stresses, respectively. The stresses can be of any kind: normal, shear and principal stresses. A further goal comes from the imposition of stability against sliding. The following form is used:

$$c_1 F_h + c_2 F_v - c_o \leq 0 \tag{12}$$

where c0,c1 and c2 are constants and Fh, Fv are the global forces in the horizontal and vertical directions, respectively.
The crest of a dam must have substantial thickness to resist the shock of floating objects, to afford a roadway and to support auxiliary structures on top of the dam.

$$t(x) \geq t^l \tag{13}$$

In the case of gravity dams, the global moment requirement must be introduced to control the overturning moment:

$$c_3 [F_h(v - v_o) - F_v(h - h_o)] - c_4 b F_v \leq 0 \tag{14}$$

where b is the thickness of the base, c3 and c4 are constants. v and h are coordinates of F_h and F_v, respectively. (h_o, v_o) are the coordinates of the point at the base of the dam on the downstream face, which is kept fixed during the optimization. On the basis of this expression it is possible to impose limits on the eccentricity of global forces:

$$e(x) \leq e^u \qquad e(x) \geq -e^u \tag{15}$$

In the case of arch dams the angle of thrust at the abutment y should exceed an allowable minimum value and the central angle of the arch f must be less than a specified value, respectively:

$$\psi \geq \psi^l \tag{16a}$$

$$\phi \leq \phi^u \tag{16b}$$

The optimization method described in the next section requires that all these goals should be casted in a normalized form.
If some reference volume $\underline{V}$ is specified, these criteria may be written in the form,

$$g_1(x) = \frac{V(x)}{\underline{V}} - 1 \leq 0 \tag{17a}$$

$$g_2(x) = \frac{\sigma(x)}{\sigma^u} - 1 \leq 0 \tag{17b}$$

$$g_3(x) = \frac{\sigma(x)}{\sigma^l} + 1 \leq 0 \tag{17c}$$

$$g_4(x) = c_1 F_h(x)/c_o + c_2 F_v/c_o - 1 \leq 0 \tag{17d}$$

$$g_7(x) = -\frac{t}{t^l} + 1 \leq 0 \tag{17e}$$

and for gravity dams:

$$g_5(x) = -\frac{e(x)}{e^u} - 1 \le 0 \qquad (17f)$$

$$g_6(x) = -\frac{e(x)}{e^l} + 1 \le 0 \qquad (17g)$$

Alternatively, for arch dams:

$$g_5(x) = -\frac{\psi}{\psi^l} + 1 \le 0 \qquad (17f)$$

$$g_6(x) = \frac{\phi}{\phi_v} - 1 \le 0 \qquad (17g)$$

The objective is to minimize all these goals over shape variables x. This is achieved by solving the minimax optimization problem:

$$\text{Min}_x \ \text{Max}\, j\,(g_1, \ldots, g_j \ldots g_7) = \text{Min}_x \ \text{Max}_{j=1,7} < g_j(x) > \qquad (18)$$

Different weights can be attributed to different goals just by changing the reference volume, tipping moments, stress or eccentricity limits. The objective of this Pareto optimization is to obtain an unbiased improvement of the current design. This minimax problem is discontinuous and non-differentiable, both of which attributes make its numerical solution by direct means difficult. Simões and Templeman (1989) have shown that the minimax solution may be found indirectly by the unconstrained optimization of a scalar function,

$$\text{Min}_x \left(1/\pi\right) \log \left\{ \Sigma_{j=1,m} \exp\left[r\, g_j(x)\right] \right\} \qquad (19)$$

with a sequence of values of increasingly large positive $p \ge 1$.

4.4 Scalar Function Optimization

Problem (19) is unconstrained and differentiable which, in theory, gives a wide choice of possible numerical solution methods. However, since the goal functions $g_j(x)$ do not have explicit algebraic form in most cases, the strategy adopted was to solve (19) by means of an iterative sequence of explicit approximation models. An explicit approximation can be formulated by taking Taylor series expansions of all the goal functions $g_j(x)$ truncated after the linear term. This gives:

$$\text{Min} \left(1/\rho\right) \log \left\{ \Sigma_{j=1,7} \exp \rho\left[g_j(x_o) + \Sigma_{j=1,N} \frac{\partial g_j(x_o)}{\partial x_i} (x_i - x_o)\right] \right\} \qquad (20)$$

Problem (20) is now an explicit approximation to problem (19) if values of all $g_j(x_o)$ and $\partial g_j(x_o)/\partial x_i$ are known numerically. Given such values (20) can be solved directly by any standard unconstrained optimization method. Solving (20) for particular numerical values of $g_j(x_o)$ and $\partial g_j(x_o)/\partial x_i$ forms only one iteration of the complete solution of problem (19). The solution vector x1 of such an iteration represents a new design which gives new values for $g_j(x_o)$ and $\partial g_j(x_o)/\partial x_i$ to replace those corresponding to x_o. Iterations

continue until changes in the design variables become small. The minimax optimization algorithm requires a sequence of positive values of ρ increasing towards infinity. This user-specified parameter controls the closeness of the envelope is to the original constraints and objective functions. An initial value of 30 increasing to 100 in subsequent iterations usually works well in this type of problems.
For the analysis model, the strategy followed during the sequential minimization process in this work was to initially employ a fairly refined mesh in the time domain to define the discretized parametric functions. After completion of the first optimization process, a more highly refined time mesh was used to test whether or not the the current design was feasible.
Sensitivity analysis consists of the evaluation of values for the derivatives of the goal functions and will be considered later.

4.5 Internal Force Approximation

Since the relationship between the stresses and design variables is highly nonlinear and considering the fact that the variation of the internal force is gradual, it is suggested that the internal forces at the control points be represented in the vicinity of x_o by the affine terms of a Taylor series:

$$F_j(x) = F_j(x_o) + \Sigma_{i=1,N} \frac{\partial g_j(x_o)}{\partial x_i} (x_i - x_o) \qquad (21)$$

The internal forces having been determined by (21), stresses at the control points of the dam can be calculated by the formulas of the strength of materials theory. Experience shows that replacing the stresses given by (7) by the internal forces convergence is smoother and faster to an optimum solution.

5. SENSITIVITY ANALYSIS

Design sensitivity analysis, that is, the calculation of quantitive information on how the response of a structure is affected by changes in the variables that define its shape, is a fundamental requirement for shape optimization. The first partial derivatives of structural response quantities with respect to shape variables provide the essential information required to couple mathematical optimization methods with structural analysis procedures. The computation of this information is often the major computational cost of the optimization process. Finite differences can be employed as a last resort or if the number of design variables is small. If forward finite differences are chosen the number of complete structural analysis required for the sensitivity analysis computations in each iteration equals the number of design variables. Care has to be taken to select an appropriate step size to reduce both truncation and condition (round-off and algorithmic) errors. If no step-size gives acceptable errors, a very inefficient central difference approximation might be used at a cost of 2 n analysis.

5.1 Discrete Analytical and Semi-analytical Sensitivity

Two general approaches are used for computing sensitivities more efficiently: differentiation of the continuum equations followed by discretization, and the reverse approach of discretization followed by differentiation. The method described in this section belongs to the latter class. The analytical expressions for sensitivity analysis are derived by differentiating (5) with respect to x_j:

$$\frac{\partial_u}{\partial x_i} = K^{-1} \left[\frac{\partial P}{\partial x_i} - \frac{\partial K}{\partial x_i} u \right] = K^{-1} \lambda P \qquad (22)$$

where,

$$\lambda P = \Sigma_e \left[\frac{\partial P_e}{\partial x_i} - \frac{\partial K_e}{\partial x_i} u_e \right] \tag{23}$$

represents a pseudo-load matrix. Then, differentiating (6) and (7) with respect to x_i:

$$\frac{\partial R}{\partial x_i} = Q K^{-1} \lambda_F \tag{24}$$

$$\frac{\partial \sigma}{\partial x_i} = \frac{\partial S_e}{\partial x_i} u_e + S_e \left(K^{-1} \lambda_p \right) e \tag{25}$$

where Q, S and K are functions of x. Analytical methods are the most efficient and accurate, but knowledge of the source code used for the structural analysis is compulsory. The derivatives of the stiffness matrix $\delta K/\delta x_i$ and the pseudo load $\delta Q/\delta x_i$ are obtained through very careful and lengthy derivation.
The semi-analytical method is based on finite difference evaluations of the derivatives of the stiffness matrix and load vector and most of this information can be extracted from a commercialy available code. The semi-analytical method for sensitivity analysis consists of the following steps:

1. - Given a proper step length vector $\Delta x_i = (0, 0, \ldots, \Delta x_i, \ldots, 0)$, the difference approximation of pseudo-load vector Qp is:

$$Q_p = S_{e \in E} \left(-K_e(x + \Delta xi)\, u + K_e(x)\, u + P_e(x + \Delta xi) - P_e(x) \right) / \Delta x_i \tag{26a}$$

where subscript e denotes the eth element and E is the set of elements related to the design variable xi.

2. - Finding $\partial u/\partial x_i$ from,

$$\partial_u/\partial x_i = K^{-1} Q_p \tag{26b}$$

3. - Evaluating the first-order approximation of displacement at design $x+\Delta x_i$,

$$u(x+\Delta xi) \cong u(x) + \partial u/\partial x_i\, \Delta x_i \tag{26c}$$

4.- Obtaining the sensitivity of the response by local differences:

$$\partial R/\partial x_i \cong [\, R(x+\Delta x_i,\, u+\Delta u) - R(x,u) \,] / \Delta x_i \tag{26d}$$

5.2 Dynamic Sensitivities

The method of modal superposition used for dynamic stress analysis requires the sensitivities of the natural modes of the dam. Formulas for computing the sensitivities of natural modes for a nonsymmetrical matrix are derived next. The eigenvalue problem (9) is guaranteed to have real distinct solutions in dam shape optimization. Moreover, a good approximation to the mode shape can be obtained with a relatively small number of terms.

Mode acceleration procedures (Sutter et al., 1988) can also be used to improve convergence. The gradients of displacements can be obtained by differentiation of equation (9) with respect to xi:

$$\frac{\partial u}{\partial x_i} = \frac{\partial}{\partial x_i} \Sigma_r q_r \varnothing_r = \Sigma_r \left[q_r \frac{\partial \varnothing_r}{\partial x_i} + \frac{\partial q_r}{\partial x_i} \varnothing_r \right] \tag{27}$$

But, to compute (îqr/îxi), the quantities:

$$\frac{\partial \omega_r}{\partial x_i} = \frac{1}{2} \frac{\partial \lambda_r}{\partial x_i} - 2\mu_r \frac{\partial \mu_r}{\partial x_i} \left(\lambda_r - \mu_r^2 \right) - \frac{1}{2} \tag{28a}$$

and,

$$\frac{\partial \mu_r}{\partial x_i} = \varnothing_r^t C \frac{\partial \varnothing_r}{\partial x_i} + \frac{1}{2} \varnothing_r^t \frac{\partial C}{\partial x_i} \varnothing_r \tag{28b}$$

are needed. It will be noted that the calculation of gradients of the eigenvalues and the eigenvectors is indispensable for the evaluation of the right-hand sides of equations (27) through (28). These calculations are discussed next (Nelson, 1976). Differentiating both sides of the eigenvalue equation with respect to each variable xi gives:

$$\left[K - \lambda_r M \right] \frac{\partial \varnothing r}{\partial x_i} + \left(\frac{\partial K}{\partial x_i} - \lambda_r \frac{\partial M}{\partial x_i} \right) \varnothing_r - \frac{\partial \lambda_r}{\partial x_i} M \varnothing_r = 0 \tag{29}$$

Pre-multiplying equation (41) by Ort and making use of the symmetry of M and K leads to the calculation for gradients of eigenvalues:

$$\frac{\partial \lambda_r}{\partial x_i} = \varnothing_r^t \frac{\partial K}{\partial x_i} - \lambda_r \frac{\partial M}{\partial x_i} \varnothing_r \tag{30}$$

Compared with modal analysis, constraints arising in the step-by-step integration procedure depend on one additional parameter: time. The constraints must be satisfied from the initial to some final time. For actual computations, the constraints must be discretized at a series of time points. The distribution of time points has to be dense enough to preclude the possibility of significant constraint violation between time points. This type of constraint discretization can greatly increase the number of constraints and thus the cost of optimization. Therefore it is desirable to find ways to remove the time dependence without substantially increasing the number of constraints. The use of envelope functions is one way to to reduce the number of constraints handled by the optimizer and making it more efficient, as it has been explained in the multi-objective formulation. However, for linear systems a step-by-step dynamic analysis is always more costly than the modal supperposition method.

6. EXAMPLE

The follwing problem has been chosen to illustrate the optimization procedure. The gravity dam is 100 m height and has 6 m minimum thickness. The compressive and tensile strengths of the concrete are 10,000 kN/m2 and 1,000 kN/m2, respectively. Elastic properties:

$E=2.1\ 10^7\ kN/m^2$; $\nu = 0.2$; body forces $2.4\ 10^7\ kN/m^2$

Foundation properties:

$E = 10^7 kN/m^2$; $\nu = 0.15$

The load combinations are: 1) dead weight; 2) self weight, water pressure, uplift; 3) dead weight, water pressure, uplift, earthquake; 4) dead weight, earthquake.

The safety factor for load conditions 1) and 2) is 2.5. The tensile stresses in the air and water faces are 400 kN/m^2 and $hq-400 \leq 0$, respectively, where h is the weight below water and q is the unit water weight. Safety against sliding is guaranteed if $V\ 0.8/H \geq 1.5$, where V and H are the sums of vertical and horizontal forces, respectively. Safety against overturning requires that the eccentricity of the resulting force e should be $|e| \leq 1/6$.

The safety factor for load conditions 3) and 4) is 1.92. The tensile stresses in the air and water faces are 520 kN/m^2 and $hq-520 \leq 0$, respectively. Safety against sliding is guaranteed if $V\ 0.8/H \geq 1.2$. Safety against overturning requires that the eccentricity e should be $|e| \leq 1/3$. Energy dissipation in the structure is represented by constant hysteretic damping. An equivalent damping ratio of 0.05 is considered.

Seismic effects are computed by standard static forces and dynamic analysis. Fig.10 represents the maximum tensile stresses that arise during an earthquake when the initial shape is considered. This shape is inadequate because the tensile stresses largely exceed their allowable values.

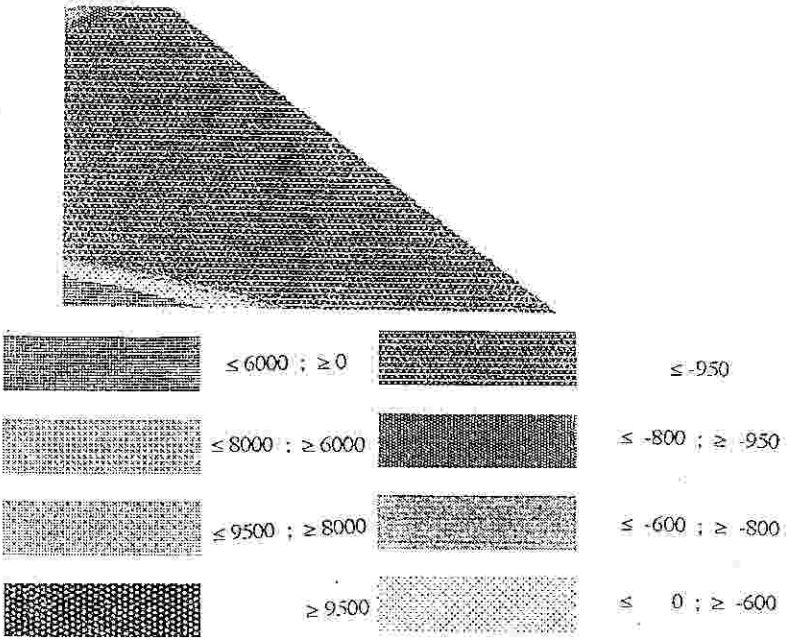

Fig. 10 Maximum Compressive and Tensile Stresses

Sliding, overturning and minimum thickness at the top are the critical goals in the static approach. This design fails to predict the large tensile stresses that arise in the downstream face. Tensile stresses 2.5 times larger than the allowable values were found when the "static" optimal shape was analysed by the linear dynamic routine. Consequently, stress requirements are critical in finding optimal shapes on the basis of

linear dynamic behaviour. Moreover, these tensile stresses cause a large increase in the volume of concrete. Fig.11 shows the shapes and corresponding maximum tensile stresses obtained for the linear dynamic approach after 1 and 3 iterations, respectively, and for the 3 and 5 variable representation.

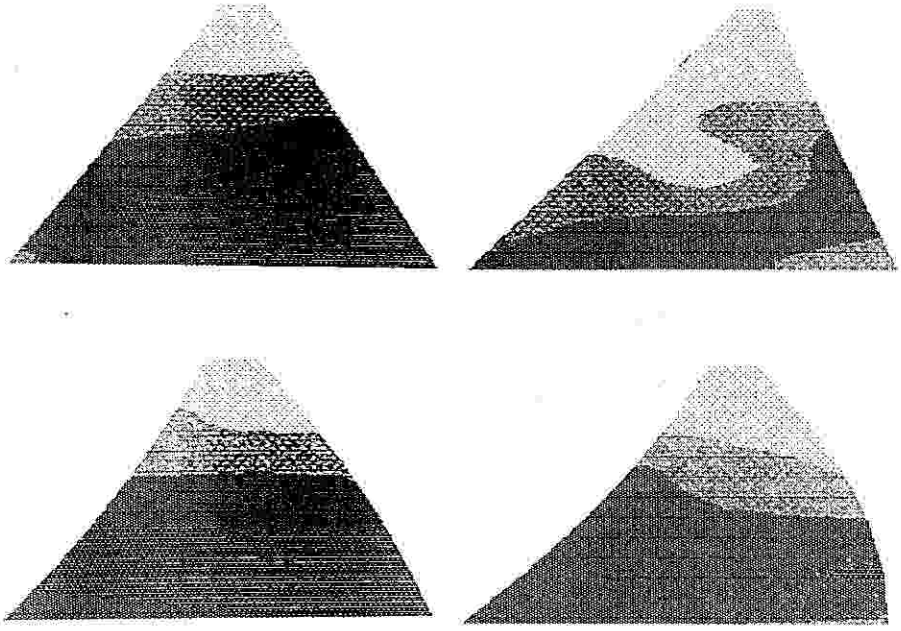

Fig. 11

Fig.12 represents the solution obtained after 2 iterations when a elastoplastic Mohr-Coulomb yield criterion is used to model the concrete behaviour. The elastoplastic model gives a more economical design by reducing the concrete volume by approximately 13%.

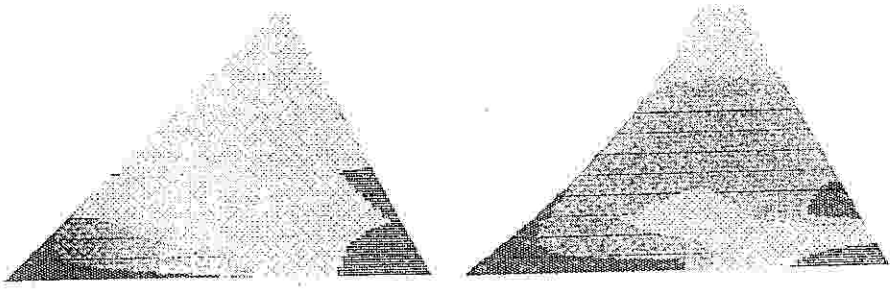

Fig. 12

The optimal geometries are shown in Figure 13. Because of increasing flexibility of describing the shape of the dam, the volume may be reduced by increasing the number of design variables. The volume reduction is due to the increase in the vertical component of water pressure.

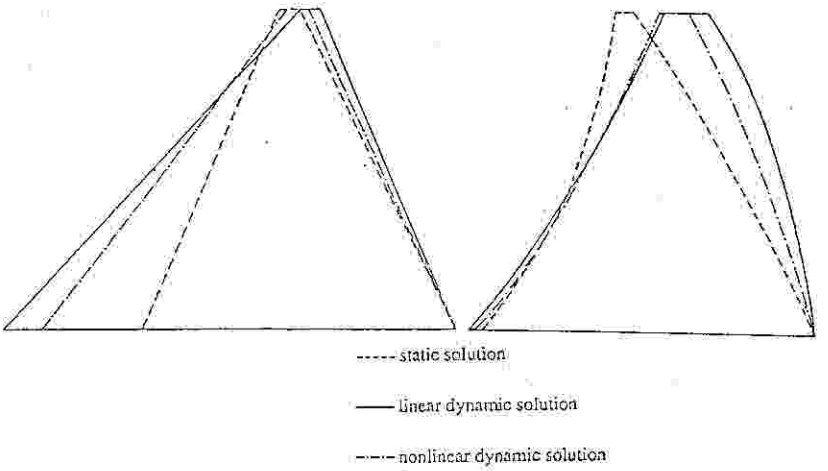

Fig. 13 Optimal geometries

The first complete optimization was performed using a mesh time interval equal to one-eigth of the fundamental period of the initial design. For the final refined mesh a time interval equal to one-eigth the third mode period for the current design was employed. Maximum tensile stresses in the air face are dominant when the dynamic response is considered. These tensile stresses cause a substantial increase in concrete volume. The concrete volume can nevertheless be reduced by using a nonlinear model.

REFERENCES

RAMAKRISHNAN, C.V. and A. FRACAVILLA (1975)
Structural Shape Optimization using Penalty Functions, J.Struct. Mech. 3, 403-422.

VITIELLO, E. (1973)
Shape Optimization using mathematical Programming and Modelling Techniques, Second Symposium on Structural Optimization, AGARD Conf. Poc. CP-123, Milan, Italy.

FIALHO, J.F.L. (1955)
Leading principles for the design of arch dams - a new method of tracing and dimensioning, LNEC, Lisbon, Portugal.

SHARPE,R.(1969)
The optimum design of arch dams, Institution of Civil Engineers, Paper 7200S.

WASSERMAN, K. (1983-84)
Three dimensional shape optimization of arch dams with precribed shape functions, J. Struct. Mech., 11 (4), pp.465-489.

RICKETTS, R.E. and ZIENKIEWICZ, O.C. (1984)
Shape Optimization of Continuum Structures, New Directions in Optimum Structural Design (Ed. E. Atreck, R.H. Gallagher, K.M.Ragsdell and O.C. Zienkiewicz) J. Wiley, NY, pp. 139-166.

ZHU BOFANG (1987)

Shape Optimization of Arch Dams, Water Power and Dam Construction, Sept., 42
TSAI, C.S. (1992).
Semi-Analytical Solutions for Hydrodynamic pressure on Dams with Arbitrary Upstream Face Considering Water Compressibility, Comp. Structures 42, 497-502
SIMÕES, L.M.C. and TEMPLEMAN, A.B. (1989)
Entropy-based Synthesis of Pretensioned Cable Net Structures, Engrg. Optimization 15, 121-140.
SUTTER, T.R., CAMARDA, C.J., WALSH J.L. and ADELMAN, H.M. (1988)
A Comparison of Several Methods for the Calculation of Vibration Mode Shape Derivatives, AIAA Journal 26,1506-1511.
NELSON, R.B. (1976)
Simplified Calculation of Eigenvector Derivatives, AIAA Journal 14, 1201-1205.